

**Organization of Bacteriochlorophylls in individual Chlorosomes from *C. tepidum*  
Studied by 2-Dimensional Polarization Fluorescence Microscopy<sup>#</sup>**

*Yuxi Tian<sup>†</sup>, Rafael Camacho<sup>†</sup>, Daniel Thomsson<sup>†</sup>, Michael Reus<sup>‡</sup>, Alfred R.  
Holzwarth<sup>\*,‡</sup> and Ivan G. Scheblykin<sup>\*,†</sup>*

<sup>†</sup> Chemical Physics, Lund University, Box 124, 22100, Lund, Sweden;

<sup>‡</sup> Max-Planck-Institut für Bioanorganische Chemie, D-45470 Mülheim an der Ruhr,  
Stiftstr. 34-36, Germany

\* E-mail corresponding authors: Ivan.Scheblykin@chemphys.lu.se

holzwarth@mpi-muelheim.mpg.de

**1. Concentration dependence**

As shown in **Figure S1**, at low concentrations, the number of chlorosomes per image is linear against the concentration. However, at higher concentrations, deviation from the linear dependence was observed. Aggregation and overlapping of individual molecules can be the reasons of this deviation. Therefore, we worked at relatively low concentration within the linear range.

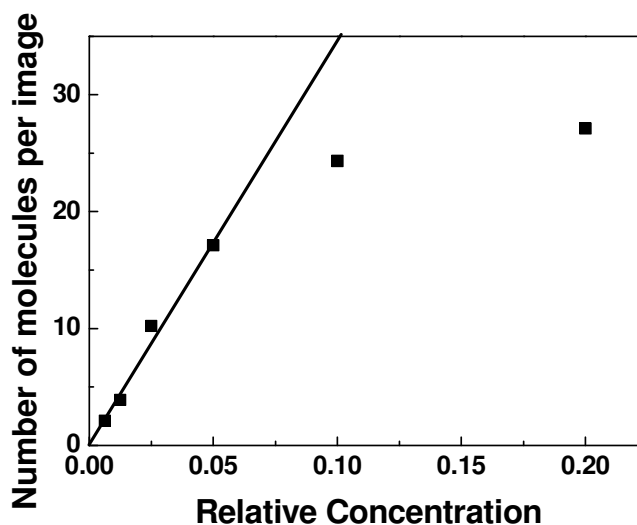


**Figure S1** Concentration dependence of the number of fluorescence spots per image at a constant

excited sample area (9 images were used for each concentration).

## 2. Detailed description of 2D-polarization single molecule imaging

2-dimensional polarization imaging of individual chlorosomes was performed using the set-up as described previously<sup>1</sup>. Briefly, as shown in **Figure 02**, a  $\lambda/2$  waveplate is placed into the linearly polarized excitation beam and a wire-grid polarizer (analyzer) was placed in front of the CCD camera. A band pass filter (transmission band 750-770 nm) is used to cut off the emission from BChl a. A Berek polarization compensator is used to maintain the linear polarization of the excitation light at the sample plane which otherwise is elliptical due to the dichroic mirror. By rotating the  $\lambda/2$  plate with a stepping motor, the polarization angle of the excitation light ( $\varphi_a$ , where “a” stands for absorption) is rotated in the sample plane. The analyzer orientation angle ( $\varphi_f$ , where “f” stands for fluorescence) is also rotated independently by another stepping motor with a lower frequency. The fluorescence was separated into two channels (reflection ( $I_R$ ) and transmission ( $I_T$ )) by the analyzer. Both channels were recorded simultaneously by the CCD camera as shown in **Figure S2a**. By analyzing the data from these two channels, the fluorescence intensity  $I(\varphi_a, \varphi_f)$  as a function of angles  $\varphi_a$  and  $\varphi_f$  is obtained (**Figure S2b**). This two-dimensional function,  $I(\varphi_a, \varphi_f)$ , contains all information about the linear polarization properties of the investigated particle. All the modulation depth and phase shift data were obtained by fitting of this two-dimensional function (see ref. 1 for detailed fitting procedure). If the fluorescence quantum yield is independent of the excitation polarization (which is a reasonable assumption) the fluorescence intensity as a function of  $\varphi_a$  is directly proportional to the absorption of the excitation light polarized at angle  $\varphi_a$ . Therefore, for the sake of simplicity, we will subsequently use the term “polarization properties in absorption” rather than “polarization properties in fluorescence excitation”.

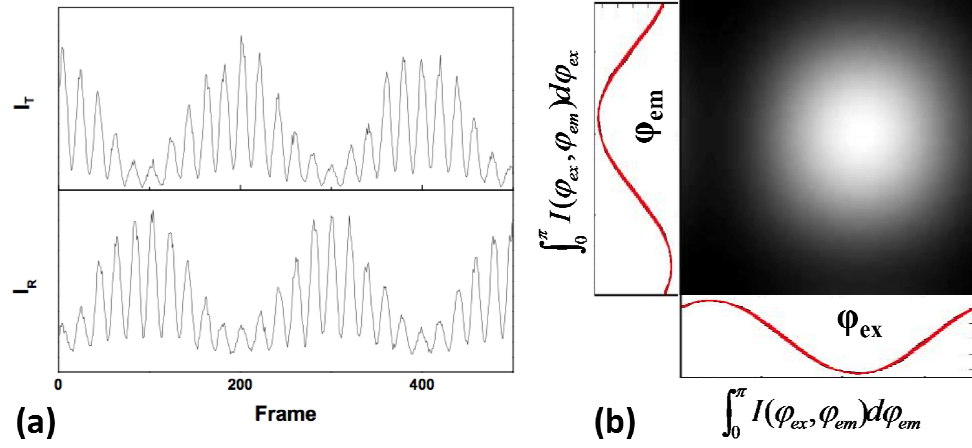


**Figure S2** An example of 2D polarization data obtained for an individual chlorosome: (a) fluorescence intensity trace measured in the transmission ( $I_T$ ) and the reflection ( $I_R$ ) channels; (b) 2D polarization plot ( $I(\varphi_a, \varphi_f)$ ). The curves to the left and below the 2D plot show  $I(\varphi_a, \varphi_f)$  integrated over  $\varphi_a$  and  $\varphi_f$ , respectively.

To illustrate the method let us consider a system containing two dipole transitions for both absorption and fluorescence. The dipoles can be different in absorption ( $d_{a1}$ ,  $d_{a2}$ ) and fluorescence ( $d_{f1}$ ,  $d_{f2}$ ) due to e.g. energy transfer (**Figure S3**). By integration of the fluorescence intensity  $I(\varphi_a, \varphi_f)$  over one of the angles as shown in **Figure S2**, we can get the angular dependences  $I(\varphi_a)$  and  $I(\varphi_f)$ . The modulation depth ( $M_a$  and  $M_f$ ) is calculated by the equation given in **Figure S3**. We define  $\theta_a^0$  and  $\theta_f^0$  as the absorption and fluorescence phases, respectively. The difference between  $\theta_a^0$  and  $\theta_f^0$  is referred as the phase shift ranging from  $-90^\circ$  to  $90^\circ$ . The phases ( $\theta_a^0$  and  $\theta_f^0$ ) depend on the contributions of all individual transition dipoles and, in a complex arrangement of chromophores, do not necessarily coincide with any of the individual chromophore transition dipole directions, as illustrated in **Figure S3**.

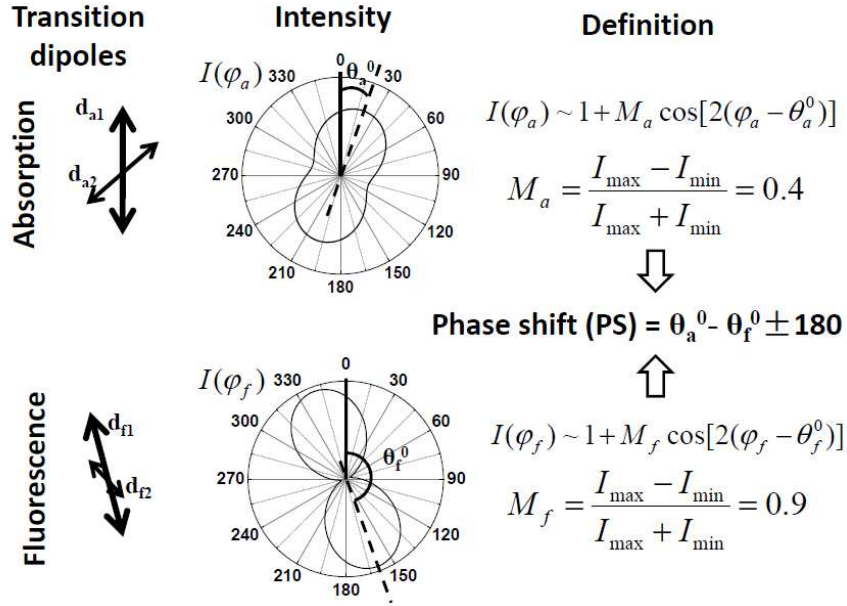


**Figure S3** Definition of the parameters obtained by the 2D polarization single molecule spectroscopy technique.

In our experiments the sample plane is parallel to the XY plane and the Z axis coincides with the optical axis of the microscope. The numerical aperture of the objective lens (NA=0.65) is low enough to allow disregarding the excitation and detection of transition dipole components parallel to the Z axis. Thus for 3-D objects we only need to consider the projection of all the transition dipoles on to the sample plane (i.e. the XY plane). Therefore the definition of the experimental parameters is the same as in the 2-D situation (**Figure S3**).

In our setup the dichroic mirror is tilted by  $45^\circ$  to the incident fluorescence light. Therefore, if the polarization plane of a linearly polarized light is not exactly parallel or perpendicular to the tilting axis of the dichroic mirror the light becomes elliptically polarized after passing through it. The depolarization depends on the polarization angle, the particular mirror and the wavelength. Since the fluorescence is not monochromatic, a Berek compensator cannot be used for correction. Thus we used a special correction procedure to correct the depolarization effect, which is described below.

In order to measure the extent of the depolarization we measured with the same detection system as for the real 2D experiments the modulation depth  $M_f$  and the emission phase  $\theta_f$  of a linearly polarized fluorescence light ( $M_f = 1$ ) provided by a

1 device which we call “artificial molecule” with a given polarization orientation  
 2 (absorption phase  $\theta_a$ ) in the sample plane XY. As shown in Figure S4, the “artificial  
 3 molecule” consisted of a polarizer placed instead of a single molecule sample and a  
 4 concentrated solution of chlorosomes placed on top of the polarizer (the chlorosome  
 5 solution is only needed to produce fluorescence light in the same spectral range as the  
 6 real sample of individual chlorosomes). Circular polarized excitation light was used to  
 7 excite the sample. The fluorescence of the chlorosome solution after passing through  
 8 the polarizer become linearly polarized (modulation depth  $M_f = 1$ ) and was collected  
 9 by the objective lens. By rotating the polarizer in the sample plane we could study the  
 10 depolarization effect of the whole light collecting system as a function of the  
 11 “artificial molecule” orientation (or absorption phase)  $\theta_a$ . If no depolarization is  
 12 introduced the measured modulation depth  $M_f$  should be 1 and the measured emission  
 13 phase  $\theta_f$  should be equal to the absorption phase  $\theta_a$ . The values of  $M_f$  and  $(\theta_f - \theta_a)$   
 14 showed clear correlations with the orientation of the “artificial molecule” (angle  $\theta_a$ ).  
 15 Obviously, such correlations are the consequence of depolarization effects in the  
 16 optics of the microscope. The modulation depth was reduced by up to 20% and the  
 17 phase shift up to 15 degrees for certain orientations of the artificial molecule. For the  
 18 angles  $\theta_a$  equal to 0 and 90 degrees the measured parameters were equal to the  
 19 expected ones indicating that no depolarization effect for these particular orientations  
 20 occurred. Obviously such correlations should be removed from the experimental data,  
 21 which was done both for the modulation depth and the phase shift.

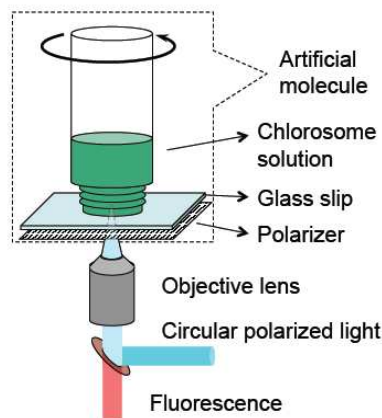


**Figure S4.** “Artificial molecule” for the polarization artifact correction

### 3. 2D results for WTLL chlorosomes

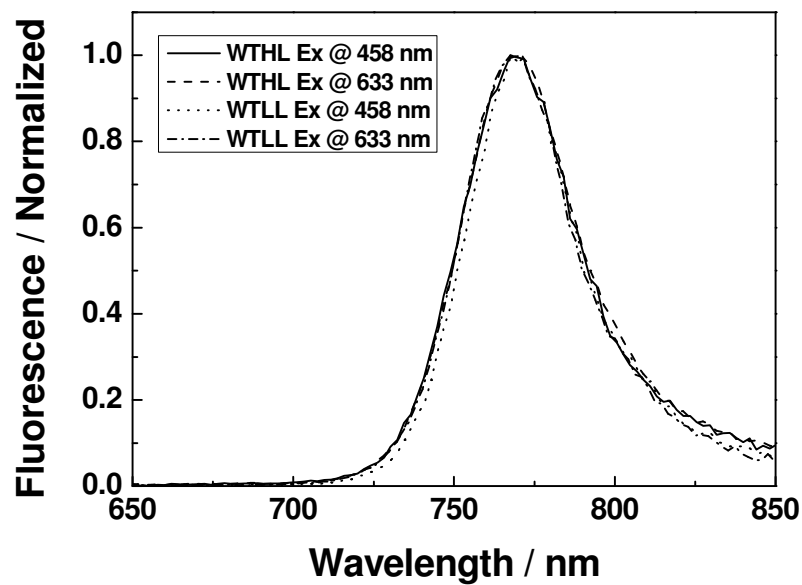


**Figure S5** Fluorescence spectra of individual WTLL chlorosomes when excited at 458 nm and 633 nm (as indicated).

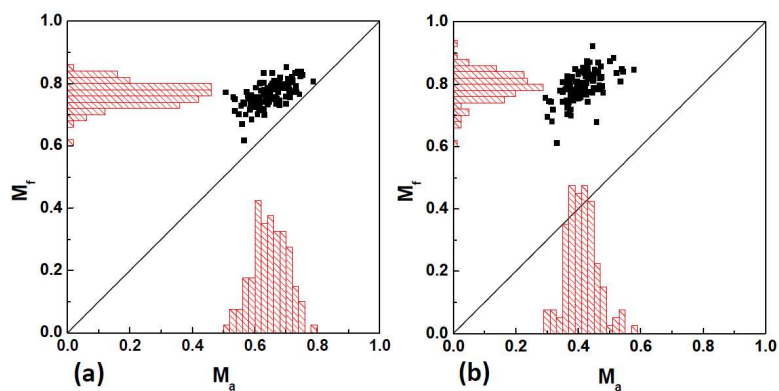


**Figure S6** Histograms and correlation between fluorescence ( $M_f$ ) and absorption ( $M_a$ ) modulation depth of WTLL chlorosomes when excited at 458 nm (a) and 633 nm (b).

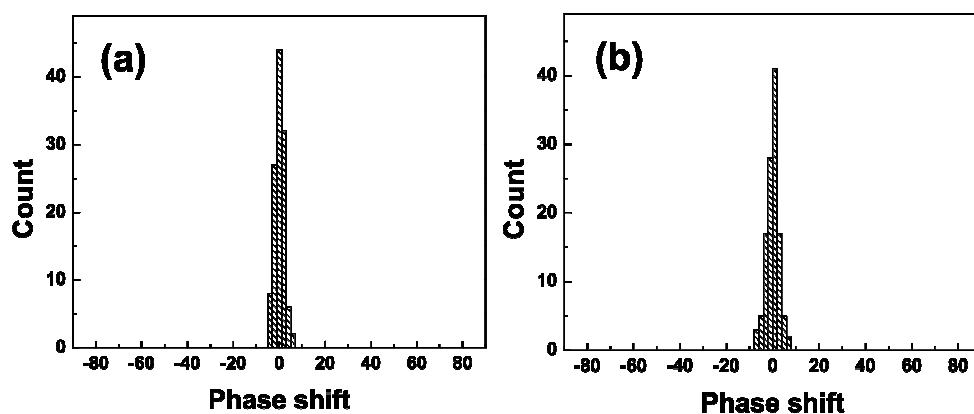


**Figure S7** Histogram of Phase shift of the WTLL chlorosomes when excited at 458 nm (a) and 633 nm (b).

#### Reference List

1. Mirzov, O.; Bloem, R.; Hania, P. R.; Thomsson, D.; Lin, H. Z.; Scheblykin, I. G. Polarization Portraits of Single Multichromophoric Systems: Visualizing Conformation and Energy Transfer. *Small* **2009**, 5 (16), 1877-1888.